

# Study on mixing characteristics in shaken microwell systems

Yi Li<sup>a</sup>, Andrea Ducci<sup>b</sup>, Martina Micheletti<sup>a,\*</sup>

<sup>a</sup>*Bernard Katz Building, Department of Biochemical Engineering, University College London, Gower Street, London, WC1E 6BT, United Kingdom*

<sup>b</sup>*Department of Mechanical Engineering, University College London, Torrington Place, London, WC1E 7JE, United Kingdom*

---

## Abstract

Shaken microwell plates are widely used for early bioprocess development as they allow a large number of experiments to be performed in parallel by using small amount of materials. Despite their widespread use, microwell plates have not been characterised from an engineering viewpoint. In this study, mixing time measurements were carried out in two wells of square and cylindrical cross sections for small orbital diameter shaker,  $d_o=3$  mm, commonly used in commercial microwell platforms (i.e. ThermoMixer) and compared against measurements obtained in lab scale reactors for larger orbital diameters. The Dual Indicator System for Mixing Time (DISMT) method was employed for all the operating conditions investigated, and a range of rotational speeds was identified where mixing is less effective due to reduced free surface oscillation. An effective scaling parameter between microwell platforms and lab scale reactors was identified based on the natural frequency of the system, which depends only on fill volume, size and cross section of the reactor.

## Highlights

- Reduced free surface oscillation leads to reduced mixing time in square microwell geometry.

---

\*Corresponding author

*Email address:* [m.micheletti@ucl.ac.uk](mailto:m.micheletti@ucl.ac.uk) (Martina Micheletti)

- 1  
2  
3  
4  
5  
6  
7  
8  
9  
10  
11  
12  
13  
14  
15  
16  
17  
18  
19
- Surface tension plays a critical role in the mixing process in square microwell plates.
  - Mixing times are longer in cylinder wells at low shaken speeds when compared to square microwells.
  - Natural frequency is a promising scaling parameter for microwells and larger reactors.

20  
21  
22  
23  
24  
25  
26  
27  
28  
29  
30  
31  
32  
33  
34  
35  
36  
37  
38  
39  
40  
41  
42  
43  
44  
45  
46  
47  
48  
49  
50  
51  
52  
53  
54  
55  
56  
57  
58  
59  
60  
61  
62  
63  
64  
65

*Keywords:* Mixing, Orbitally shaken reactors, Mixing time, Microwells, Dual indicator method, Scaling

---

1  
2  
3  
4  
5  
6  
7  
8  
9 **1. Introduction**

10  
11 Bioreactors are used for growing organisms such as bacteria, yeast and mam-  
12 malian cells under controlled operating conditions. For screening and process  
13 development studies at the lab scale, Orbitally Shaken Reactors (OSRs), such  
14 as Erlenmeyer flasks and microwell plates, are commonly employed. At larger  
15 scale, Stirred Tank Reactors (STRs) that rely on the use of stirrers to create  
16 correct fluid motion are the most common geometries. Due to the prevalence  
17 of STRs in the chemical and biochemical industries, several studies can be  
18 found in the literature that provide a thorough investigation of their mixing  
19 and fluid dynamics characteristics for a broad range of operating conditions  
20 [1, 2, 3, 4, 5, 6]. In recent years, the engineering characterisations of lab-  
21 scale OSRs have also been conducted by various researchers in terms of flow  
22 dynamics [7, 8, 9, 10, 11, 12], free surface motion [13, 14], solids suspension  
23 [15, 16] and power consumption [17, 18, 19], both experimentally and numer-  
24 ically.  
25  
26  
27  
28  
29

30  
31 Microscale technologies such as shaken microwell plates have been used ex-  
32 tensively in early stage bioprocess development for screening and process op-  
33 timisation, before the process can be implemented in conventional STRs. Un-  
34 like lab-scale OSRs which mainly comes in cylindrical geometry, microscale  
35 multi-well plates usually have square or cylindrical cross-sectional shapes and  
36 various bottom designs, such as flat, U-shaped or conical bottom. Most en-  
37 gineering characterisation studies in shaken microwell plates have focused on  
38 gas-liquid mass transfer [20, 21, 22, 23, 24] and power consumption [23, 25].  
39 For example, Doig *et al* [22] experimentally measured the volumetric oxygen  
40 transfer coefficient ( $k_L a$ ) in three round microwells for a range of shaking di-  
41 ameters and frequencies, and developed a dimensionless numbers correlation.  
42 Dürauer *et al* [25] determined the local energy dissipation rate and power in-  
43 put in 6-, 24- and 96-well plates by adapting the clay/polymer flock system  
44 and demonstrated that the hydrodynamic stress is significantly different for  
45 various microwell plate formats.  
46  
47  
48  
49

50  
51 In addition to  $k_L a$  and power consumption studies, mixing time is also widely  
52 used to characterise macro-scale mixing performance in different types of  
53 bioreactors. Accurate mixing time determination in shaken reactors is criti-  
54 cal to minimise concentration gradients that are deleterious to cell cultures.  
55 A technique based on two pH indicators was used by Tissot *et al* [26] to  
56  
57  
58  
59  
60  
61  
62  
63  
64  
65

1  
2  
3  
4  
5  
6  
7  
8  
9  
10  
11  
12  
13  
14  
15  
16  
17  
18  
19  
20  
21  
22  
23  
24  
25  
26  
27  
28  
29  
30  
31  
32  
33  
34  
35  
36  
37  
38  
39  
40  
41  
42  
43  
44  
45  
46  
47  
48  
49  
50  
51  
52  
53  
54  
55  
56  
57  
58  
59  
60  
61  
62  
63  
64  
65

measure mixing time in shaken cylindrical containers. The fastest mixing zone was found near the bottom, where mixing was mainly accomplished by diffusion. A single indicator system was used by Tan *et al* [27] to quantify mixing time in Erlenmeyer shaken flasks, and compared the results to those obtained in stirred tanks with different types of impellers. Contrary to the results obtained by Tissot *et al.* [26], they concluded that the orbital diameter does not significantly affect mixing time in shaken flasks. Rodriguez *et al.* [28] conducted mixing time measurements in OSRs and identified two mixing regimes, in-phase and out-of-phase, corresponding to the flow transition phenomenon reported by Weheliye *et al.* [9]. Their results indicated that mixing time in cylindrical reactors was also affected by feeding pipe position. For both regimes insertion was recommended close to the walls where wall boundary layer shear stresses are greater. Another study conducted by Rodriguez *et al.* [29] compared the mixing times obtained for shaken cylindrical reactors and Erlenmeyer flasks to those of STRs. The study suggested to use  $N/N_{cr}$  to account for various reactor sizes and fill volumes, rather than simply using  $N$ , as the ratio takes the presence of flow transition between in- or out-of-phase conditions into consideration. They also demonstrated that the  $Fr/Fr_{cr}$  is a useful parameter in scaling up/down between different reactor systems, where  $Fr_{cr}$  is the critical Froude number based on the rotational speed associated to the flow transition. Li *et al* [30] extended the mixing dynamics study to intermediate-sized OSRs for cylindrical and square geometries ( $d_i = 35.4$  and  $40.0$  mm, respectively) shaken in the Eppendorf ThermoMixer C with a significantly reduced orbital diameter of 3 mm, in an effort to assess the validity of scaling law identified in [29] in smaller OSRs. The acceleration mode to achieve the final shaken speed in the cylindrical reactor was found to greatly affect the mixing time due to difference in free surface oscillations and a new scaling parameter based on the natural frequency of the reactor was suggested as it was demonstrated to be more effective for shaken systems with very small  $d_o$ .

A review of recent mixing time studies in shaken reactors is summarised in Table 1. It is evident in Table 1 that mixing time quantification has been conducted by a number of researchers, however, the vast majority of them focused on Erlenmeyer flasks and lab-scale cylindrical reactors. Despite the wide use of microwell plates in bioprocess development, the mixing process in microwell plates was only considered by two studies [31, 23] more than a decade ago and primarily by means of CFD and intrusive experimental tech-

1  
2  
3  
4  
5  
6  
7  
8  
9 nique. The current work aims at extending the DISMT technique established  
10 for larger OSRs further down to microwell systems of different geometries for  
11 reduced shaking orbital diameter ( $d_o = 3$  mm) and to assess the effects of  
12 fluid properties (viscosity and surface tension) on mixing time. It builds  
13 upon previous studies of Rodriguez *et al* [29] and Li *et al* [30] and aims at  
14 providing a thorough understanding of the mixing process induced by orbital  
15 shaking motion in microwell plates. From this perspective, mixing time was  
16 measured in two microwells ( $d_i = 17.1$  and  $15.6$  mm, respectively) with square  
17 and cylindrical geometries, which are mimics of commercially-available mi-  
18 crotitre plates, by means of DISMT technique.  
19  
20  
21  
22

## 23 2. Materials and methods

### 24 2.1. Microwell plates and equipment

25  
26 Two single well mimics made of acrylic plastic were used, having the same  
27 geometry of one well from commercial 24 deep square well (24 DSW) and  
28 24 standard round well (24 SRW) plates, purposely made by the UCL De-  
29 partment of Chemical Engineering Workshop. The height of the cylindrical  
30 well,  $h_v$ , was increased from 17 mm (height of the original well in 24 SRW)  
31 to 44 mm to allow higher fluid volume to be assessed. The impacts of three  
32 parameters on mixing time were investigated in the square well, including  
33 fluid volume,  $V_f$ , fluid viscosities of 10 and 100 times greater than that of  
34 water ( $v/v_w = 10$  and  $100$ , respectively), and surface tension in the range of  
35  $31.8$  to  $68.4$  mNm<sup>-1</sup>. Three fill volumes ( $V_f = 3, 4$  and  $5$  mL) were used to  
36 measure mixing time in the cylindrical well and the results were compared to  
37 the square well to assess the effect of microwell geometry on mixing perfor-  
38 mance. The full geometrical details of the two wells and operating conditions  
39 investigated in this work are summarised in Table 2.  
40  
41  
42  
43  
44  
45

46 The experimental set up is shown in Figure 1, where measurements were  
47 made using an Eppendorf ThermoMixer C, with a fixed orbital diameter of  
48 3 mm. In the set up, different wells can be screwed into a plate, which  
49 is placed in the plate holder on the ThermoMixer. An extension arm was  
50 built on the plate to allow the synchronisation of the movement of the NET  
51 iCube camera and the shaker. An LED panel was fixed at the back of the  
52 plate to reduce background noises and provide uniform illumination. A 20  
53  $\mu$ L Gilson pipette, attached to a clamp stand, was used for the addition of  
54 base to initiate the chemical reaction. The clamp stand ensured the feeding  
55  
56  
57  
58  
59  
60  
61  
62  
63  
64  
65

1  
2  
3  
4  
5  
6  
7  
8  
9 location and height were consistent for each experiment. The rotational speed  
10 investigated ranged from 300 to 1000 rpm in increments of 50 rpm.  
11

## 12 *2.2. Surface tension measurement*

13  
14 The surface tension of different solutions in the square well was determined  
15 using the Wilhelmy plate principle which is considered as one of the most  
16 appropriate ring method for surface tension measurement, due to the fact  
17 that no hydrostatic correction is required. The digital KRÜSS K100 Force  
18 Tensiometer and a platinum plate ( $20 \times 10 \times 0.1$  mm) were used to obtain  
19 surface tension measurement. The solution was placed in a thermostated  
20 flask at  $25^\circ\text{C}$  and temperature was constantly monitored by a thermostat.  
21 Three repetitions were carried out for each condition with the average value  
22 being recorded. An anionic surfactant sodium dodecyl sulphate (SDS) sup-  
23 plied by Sigma Aldrich, was dissolved in de-ionised water and the desired  
24 solution concentration was obtained by successive dilutions. The initial SDS  
25 concentration in the solution was  $3.47 \times 10^{-3} \text{ molL}^{-1}$  and diluted by fac-  
26 tors of 10, 50 and 100. The surfactant concentrations and dynamic surface  
27 tension measured by the tensiometer are shown in Table 3.  
28  
29  
30  
31  
32

## 33 *2.3. DISMT technique*

34 The technique used to estimate mixing time in microscale systems was adapted  
35 from the method developed by Melton et al. [32], namely Dual Indicator Sys-  
36 tem for Mixing Time. As the name implies, two acid-base pH indicators -  
37 methyl red and thymol blue, were present in the bulk solution, which allow  
38 a direct visualisation of pH change, with fluid being red, blue and yellow for  
39 pH values less than 6.3, greater than 8 and between 6.3 and 8, respectively.  
40 The colour change of the solution was initiated by adding small amount of  
41 sodium hydroxide, where the base rapidly react with the hydrochloric acid  
42 that is already present in the bulk solution. The colour change of the solution  
43 only occur when reactants have been mixed at the molecular level for such a  
44 reaction-based technique, thus avoiding the “micromixing” phenomenon as-  
45 sociated with dilution-based techniques. The capture speed of the **iCube**  
46 **camera** is 16 frames per second, therefore allowing short mixing time, even  
47 less than 0.1 second, to be effectively determined.  
48  
49  
50  
51  
52

53  
54 The stock solution of pH indicators were prepared in 70% ethanol and the  
55 working reagent for DISMT test was prepared in de-ionised water containing  
56 thymol blue (Fisher Scientific) and methyl red (Fisher Scientific) solutions,  
57  
58

1  
2  
3  
4  
5  
6  
7  
8  
9 with percent concentrations of  $4.67 \times 10^{-3} v/v$  and  $4.26 \times 10^{-3} v/v$ , re-  
10 spectively. Sodium hydroxide was subsequently added to the well-mixed red  
11 solution in increment of 2  $\mu\text{L}$  until a bright yellow colour was obtained. The  
12 desired volume of DISMT solution was measured into the well and it was  
13 acidified initially by adding small amount of 0.075 M HCl. The solution was  
14 red at the beginning and the reaction between acid and base was initiated  
15 by the insertion of the same amount of 0.075 M NaOH after the flow in the  
16 well was fully established. Each condition was repeated ten times to reduce  
17 the statistical error and the average of the ten measurements were used as  
18 the mixing time. **The working fluid could be re-used up to three times before**  
19 **replacing it with a fresh solution.** To prepare solution with higher viscosi-  
20 ty, absolute glycerol was mixed with certain amount of de-ionised water to  
21 obtain desired fluid viscosity. The viscosity of the glycerol/water aqueous  
22 solution was determined based on the method proposed by Cheng [33]. The  
23 image processing method used in this work was the same as that used by  
24 Rodriguez et al. [29] and Li et al. [30] who measured mixing time in larger  
25 OSRs, thus allowing a more reliable and objective comparison of mixing time  
26 across different reactor scales.  
27  
28  
29  
30  
31  
32

### 33 **3. Results and discussion**

#### 34 *3.1. Mixing time in 24-DSW plate format*

35 The impact of three parameters, namely fill volume, fluid viscosity and sur-  
36 face tension, on mixing time were investigated in the square well, a mimic of  
37 the 24-DSW plate, while shaken on the ThermoMixer C with  $d_o = 3$  mm.  
38  
39  
40

41 Figure 2 shows the mixing time variation,  $t_m$ , with respect to shaken speeds  
42 for five different fill volumes, ranging from 2 to 6 mL. It should be noted that  
43 the log scale of  $t_m$  was used to allow better visualisation of the impact of fill  
44 volume on mixing time. A significant mixing time reduction (from 100 s to  
45 10 s) occurred in the lower end range of shaken speeds investigated, between  
46  $N = 300 - 400$  rpm. It is also evident that the mixing time for  $V_f = 6$  mL  
47 was approximately 3.5 times greater than that of 2 mL at the lowest speed.  
48 For shaken speeds greater than 400 rpm, the mixing process became very  
49 rapid with mixing time less than 10 seconds for all fill volumes examined.  
50 At higher speed range, it is evident that an unexpected increase in mixing  
51 time occurred at  $N = 550 - 650$  rpm for  $V_f$  ranging from 3 to 6 mL, which  
52 was more pronounced the larger the fill volume. This phenomenon occurred  
53  
54  
55  
56  
57  
58

1  
2  
3  
4  
5  
6  
7  
8  
9 earlier at  $N = 500$  rpm for the smallest fill volume investigated. Mixing  
10 time dropped again with further increase in shaken speed and no significant  
11 change was noticed afterwards.  
12  
13

14 The unexpected mixing time increase at high speed range was associated  
15 with a change in the free surface dynamics in the well and most likely results  
16 from the very small orbital shaken diameter used. To further understand  
17 this unexpected phenomenon, the non-dimensional wave amplitude,  $\Delta h/d_i$   
18 , of the free surface was measured, where  $\Delta h$  is the difference between the  
19 highest and lowest fluid height at the centre of the reactor. Figure 3 dis-  
20 plays both the  $t_m$  variation (left y-axis) and the  $\Delta h/d_i$  variation (right-axis)  
21 with increasing shaken speed in the range of 450 to 800 rpm where the un-  
22 expected mixing time increase occurred, for  $V_f = 6$  mL. It is evident that an  
23 increase in mixing time was resulted from a decrease in free surface height  
24 and vice versa. A similar phenomenon was also noticed in the work of Li  
25 et al. [30] where a direct acceleration mode affected the free surface oscilla-  
26 tions and thus the mixing time in an intermediate-sized cylindrical reactor  
27 when shaken in ThermoMixer. The reduced free surface oscillation in the  
28 square microwell is independent of acceleration modes, however, the longer  
29 mixing time at high speed range was also due to a significantly reduced free  
30 surface height.  
31  
32  
33  
34  
35  
36

37 To further elucidate the cause of the reduced free surface oscillation, the  
38 non-dimensional wave amplitude was also measured in the square well for  
39 the same fill volume (6 mL) when shaken on a lab shaker with  $d_o = 15$  mm.  
40 The results were compared to those obtained for  $d_o = 3$  mm in Figure 4 where  
41  $\Delta h/d_i$  was plotted against  $Fr$  instead of  $N$ , in order to make the two sets of  
42 results more comparable. Consistently with Figure 2, when shaken at  $d_o =$   
43 3 mm, the non-dimensional wave amplitude dropped when  $Fr$  was increased  
44 to 0.6 corresponding to 600 rpm, which is the speed for the occurrence of the  
45 mixing time increase. On the contrary, the wave amplitude exhibited a con-  
46 stant increase with shaken speed when a larger  $d_o$  was employed. Therefore,  
47 the unexpected mixing time increase in the square well has to be related to  
48 the small orbital diameter used which has a significant impact on the free  
49 surface oscillation.  
50  
51  
52  
53  
54

55 Cell culture media used in bioprocesses generally have a viscosity similar to  
56 water, however, higher viscosities might be encountered in serum-based me-  
57  
58



1  
2  
3  
4  
5  
6  
7  
8  
9 dia for cell expansion process or in high cell density cultures. The viscosity  
10 of cell culture media in the latter context increases with time due to the  
11 presence of increasing amount of biomass. To this perspective, mixing time  
12 measurements by DISMT technique were also carried out in the square well  
13 for two fluids exhibiting greater viscosity than water and the mixing time  
14 variation with increasing shaken speed is illustrated in Figure 5. For the  
15 fluid with viscosity of  $10^{-4} \text{ m}^2\text{s}^{-1}$  (100 times more viscous than water) at  
16 low shaken speed range, the mixing time showed approximately a 7-fold in-  
17 crease as shown in Figure 5. The fluid with viscosity that is 10 times greater  
18 than water also exhibited an increase in mixing time at 300 - 350 rpm but  
19 to a much lesser extent compared to the previous discussed case. At higher  
20 speed range, it is evident that the increase in mixing time also occurred for  
21 viscous fluids and was the extent was even more pronounced. It is also worth  
22 noting that the speeds at which  $t_m$  increases for water, fluid with  $10\times$  vis-  
23 cosity and fluid with  $100\times$  viscosity are 600, 650 and 700 rpm, respectively.  
24 This indicate that this mixing time increase phenomenon occurs at a higher  
25 shaken speed, the more viscous the fluid is. For viscous fluids, the increase in  
26  $t_m$  at high speed range is also resulted from a reduced free surface oscillation.

33 Additional mixing time experiments were performed to assess the effect of  
34 surface tension on mixing dynamics in the square microwell as the interfacial  
35 tension of a liquid in the well is influenced by the gas phase and the physio-  
36 chemical property of the liquid, known as the gas-liquid interface. SDS, an  
37 anionic surfactant, was added into the bulk solution and successive dilutions  
38 were performed to obtain liquid with different surface tensions. Four surfac-  
39 tant concentrations were investigated and the results were compared to pure  
40 water when the square well was filled with 3 mL of liquid. As depicted in  
41 Figure 6, the mixing time decreased with increasing surfactant concentra-  
42 tions when shaken at the lowest speed (300 rpm). It is also evident that in  
43 the presence of surfactant the unexpected increase of mixing time at high  
44 speed range,  $N = 600 - 650$  rpm, reduced by a great extent. Therefore, the  
45 reduction of surface tension with the addition of surfactant has a significant  
46 influence on the mixing dynamics in the square microwell, both at low and  
47 high shaken speeds, suggesting surface tension is a key factor that needs  
48 to be considered during orbital shaking motions, especially at small orbital  
49 diameters. It is also worth noting that the properties of the well construc-  
50 tion material influences the liquid-solid interface, thus also impacting on the  
51  
52  
53  
54  
55  
56  
57  
58  
59  
60  
61  
62  
63  
64  
65

1  
2  
3  
4  
5  
6  
7  
8  
9 surface tension as indicated in the Young equation:

$$\sigma_{V/S} = \sigma_{L/V}(\cos\theta) + \sigma_{L/S} \quad (1)$$

10  
11  
12  
13  
14 Where  $\sigma_{V/S}$ ,  $\sigma_{L/V}$  and  $\sigma_{L/S}$  are vapour-solid, liquid-vapour and liquid-solid  
15 interfacial tensions, respectively, and  $\theta$  is the contact angle between the solid  
16 and liquid phases. As suggested in Equation (1), the construction material  
17 of the microwell needs to be taken into account when assessing the effect of  
18 surface tension on mixing.  
19  
20

### 21 *3.2. Comparison of mixing time in different well geometries*

22  
23 Microwell plates with cylindrical geometry, such as the 24-SRW plate, are  
24 also commonly used for screening and process development studies. In this  
25 section, mixing time was measured in the cylindrical microwell for three dif-  
26 ferent fill volumes ( $V_f = 3, 4$  and  $5$  mL) and the results were compared with  
27 those obtained in the square well with similar dimensions to assess the effect  
28 of reactor geometry on mixing dynamics in shaken microwell systems.  
29  
30

31  
32 At low shaken speeds, the mixing process is longer in the cylindrical well than  
33 the square one when the same fill volume is considered, as shown in Figure 7.  
34 The mixing process is more efficient in the square well, most likely due to  
35 the presence of the four corners of a square well, as they acting similarly  
36 as baffles which promoting the mixing performance in bioreactors. Similarly  
37 in the cylindrical well, mixing time dropped significantly with increasing  
38 shaken speed in the low speed range (i.e. 300 - 400 rpm), while no significant  
39 change in mixing time observed for shaken speeds greater than 400 rpm and  
40 the mixing process became very rapid afterwards. It should also be noticed  
41 that contrary to the work of Li et al. [30], no difference in mixing time was  
42 identified in the cylindrical microwell when different acceleration modes was  
43 adopted.  
44  
45  
46  
47

48  
49 Nevertheless, the phenomenon of small increase in mixing time in the high  
50 speed range was not observed in the cylindrical geometry as shown in the  
51 close up of Figure 8a. The deformation of the free surface is the most vis-  
52 ible effect of orbital shaking motion and the liquid flow within a container  
53 is uniquely defined by the pattern of its free surface, thus the free surface  
54 shape was captured by the high speed camera to allow comparison between  
55 the two geometries in terms of free surface dynamics. As shown in the free  
56  
57  
58  
59  
60  
61  
62  
63  
64  
65

1  
2  
3  
4  
5  
6  
7  
8  
9 surface snapshots for the two geometries in Figure 8b, when the cylindrical  
10 well is considered, it is evident that the free surface inclination, and therefore  
11 oscillation, continuously increases with increasing speed, resulting in faster  
12 mixing. However, when the square geometry is considered, it is clear that  
13 at speeds of 650 and 700 rpm, the free surface does not show a pronounced  
14 inclination, indicating that the sloshing mechanism and, therefore the mixing  
15 process, is reduced. It is evident from the observations that the mixing pro-  
16 cess in shaken microwell systems is in close association with the free surface  
17 dynamics.  
18  
19  
20

### 21 *3.3. OSR scaling based on Froude number*

22 The mixing time measurements obtained in the two microwells as presented  
23 in Section 3.1 and 3.2, are compared to those obtained in larger OSRs ( $d_i$   
24 = 8 - 13 cm) and greater orbital diameters ( $d_o = 1.5 - 5$  cm) as previously  
25 reported by Rodriguez et al. [29]. The mixing time results between current  
26 work and [29] are comparable as the same experimental methodology and  
27 image processing algorithms were used. The comparison between different  
28 results are in an attempt to derive a more universal scaling law for OSRs  
29 with various scales, geometries and operating conditions based on the mix-  
30 ing dynamics within the reactors.  
31  
32  
33  
34

35 In the study of Rodriguez et al. [29], two dimensionless parameters, mixing  
36 number ( $Nt_m$ ) and the ratio of  $Fr/Fr_{cr}$ , were identified as effective scaling  
37 parameters for mixing time measurements obtained in their work and those  
38 presented by Tissot et al. [26] for very different reactor sizes and operating  
39 conditions. They proposed a power law relationship for scaling in the form  
40 of  
41  
42

$$43 \quad Nt_m = a \left( \frac{Fr}{Fr_{cr}} \right)^{-b} + c \quad (2)$$

44 Where a, b and c are three constants accounting for different reactor configu-  
45 rations. They found values of a, b and c of 100.7, -1.245 and 25, respectively,  
46 best fit their data with a wide range of operating conditions. The use of  
47 the critical Froude number in scaling was found to be more effective than  
48 simply using  $Fr$ , as  $Fr_{cr}$  takes the presence of flow transition between in-  
49 and out-of-phase in the OSR into account, as described in Weheliye et al. [9].  
50  
51  
52  
53  
54

55 To assess the possibility of extending the scaling law identified in Rodriguez  
56 et al. [29] to microwell systems, their results obtained in larger cylindrical  
57  
58  
59  
60  
61  
62  
63  
64  
65

reactors for five parameter combinations and the proposed power law function are plotted in Figure 9 and compared against the mixing number curves for the two microwells with square and cylindrical geometries. It is evident on Figure 9 that the model derived by Rodriguez et al. [29] tends to overpredict the  $Nt_m$  trend obtained in microwell systems, most likely due to the small orbital diameter employed that led to different fluid and mixing dynamics within the wells. Therefore, there is a need to identify another parameter to aid the scaling across different shaken systems.

#### 3.4. OSR scaling based on natural frequency

A potential scaling parameter was identified in the work of Reclari et al. [14] who demonstrated that the natural frequency of a shaken cylindrical container is directly related to the free surface oscillations. As described in Ibrahim [34], depending on the geometry of the reactor, the natural frequency could be calculated from Equation Equation (3) for upright cylinders and from Equations Equation (4) and Equation (5) for rectangular containers. It is evident from its definitions that the natural frequency only depends on the reactor size and amount of fluid inside, but independent of shaken orbital diameter.

$$\omega_{11}^2 = \frac{2G\epsilon_{11}}{d_i} \tanh\left(\frac{2\epsilon_{11}h_f}{d_i}\right) \quad (3)$$

$$\omega_{11}^2 = Gk_{mn} \tanh(k_{mn}h_f) \quad (4)$$

$$k_{11} = \pi\sqrt{\frac{8}{d_i}} \quad (5)$$

Where  $\epsilon_{11} = 1.841$  and it is the first root of the derivative of the Bessel's function of the first kind and first order.

Mixing number variation for the two microwells are plotted together with those obtained in Rodriguez et al. [29] for five conditions (three reactor sizes and three fluid heights in one reactor) in Figure 10 based on the ratio of angular velocity and natural frequency  $\omega/\omega_{11}$ . It is evident that the two datasets correlate better by using  $\omega/\omega_{11}$  as the scaling parameter rather than  $Fr/Fr_{cr}$ , most likely due to the independence of orbital diameter of natural frequency. The natural frequency was also identified as an effective parameter in Li et al. [30] who considered mixing dynamics in intermediate-sized reactors shaken at  $d_o = 3$  mm. It could therefore be concluded that

1  
2  
3  
4  
5  
6  
7  
8  
9  $\omega/\omega_{11}$  acts as a better scaling parameter for OSRs if microwell plates and  
10 reduced orbital diameter are used.  
11

#### 12 13 **4. Conclusions** 14

15 In this study, the DISMT technique for mixing time measurement has suc-  
16 cessfully been applied to microwell systems shaken with significantly reduced  
17 orbital diameter. The effects of fill volume, fluid viscosity and surface tension  
18 on mixing time were investigated in 24 DSW and the difference of mixing  
19 dynamics between square and cylindrical geometries were assessed in a Ther-  
20 moMixer with  $d_o = 3$  mm. The mixing time of the DSW showed in general  
21 the typical variation of a mixing number curve, however it was identified a  
22 range of shaken speed  $N = 600 - 650$  rpm, which was denoted by an in-  
23 creased of mixing time with speed. This phenomenon is caused by a reduced  
24 free surface oscillation over this range of speeds, which does not occur when  
25 a cylindrical geometry is considered. With a reduction of surface tension this  
26 phenomenon disappears also in the deep square well. Mixing time measure-  
27 ments obtained in this work were compared to those reported previously in  
28 lab-scale shaken reactors by Rodriguez et al. [29]. These data indicate that  
29 the natural frequency can be used as an effective parameter to scale between  
30 microwells and larger scale shaken reactors, mostly due to the independence  
31 of orbital diameter of natural frequency.  
32  
33  
34  
35  
36  
37  
38

- 39 [1] Z. Doulgerakis, M. Yianneskis, A. Ducci, On the interaction of trailing  
40 and macro-instability vortices in a stirred vessel-enhanced energy levels  
41 and improved mixing potential, Chemical Engineering Research and  
42 Design 87 (2009) 412–420.  
43  
44 [2] Z. Doulgerakis, M. Yianneskis, A. Ducci, On the manifestation and  
45 nature of macroinstabilities in stirred vessels, AIChE Journal 57 (2011)  
46 2941–2954.  
47  
48 [3] A. Ducci, M. Yianneskis, Direct determination of energy dissipation in  
49 stirred vessels with two-point lda, AIChE Journal 51 (2005) 2133–2149.  
50  
51 [4] A. Ducci, M. Yianneskis, Vortex tracking and mixing enhancement in  
52 stirred processes, AIChE Journal 53 (2007) 305–315.  
53  
54  
55  
56  
57  
58

- 1  
2  
3  
4  
5  
6  
7  
8  
9 [5] R. Escudié, A. Liné, Experimental analysis of hydrodynamics in a radi-  
10 ally agitated tank, *AIChE Journal* 49 (2003) 585–603.  
11  
12 [6] M. Yianneskis, Z. Popiolek, J. Whitelaw, An experimental study of the  
13 steady and unsteady flow characteristics of stirred reactors, *Journal of*  
14 *Fluid Mechanics* 175 (1987) 537–555.  
15  
16 [7] J. Gardner, G. Tatterson, Characterization of mixing in shaker table  
17 containers, *Biotechnology and Bioengineering* 39 (1992) 794–797.  
18  
19 [8] H. M. Kim, J. P. Kizito, Stirring free surface flows due to horizontal cir-  
20 culatory oscillation of a partially filled container, *Chemical Engineering*  
21 *Communications* 196 (2009) 1300–1321.  
22  
23 [9] W. Weheliye, M. Yianneskis, A. Ducci, On the fluid dynamics of shaken  
24 bioreactors—flow characterization and transition, *AIChE Journal* 59  
25 (2013) 334–344.  
26  
27 [10] A. Ducci, W. H. Weheliye, Orbitally shaken bioreactors—viscosity ef-  
28 fects on flow characteristics, *AIChE Journal* 60 (2014) 3951–3968.  
29  
30 [11] E. Mancilla, C. Palacios-Morales, M. Córdova-Aguilar, M. Trujillo-  
31 Roldán, G. Ascanio, R. Zenit, A hydrodynamic description of the flow  
32 behavior in shaken flasks, *Biochemical Engineering Journal* 99 (2015)  
33 61–66.  
34  
35 [12] W. H. Weheliye, N. Cagney, G. Rodriguez, M. Micheletti, A. Ducci,  
36 Mode decomposition and lagrangian structures of the flow dynamics in  
37 orbitally shaken bioreactors, *Physics of Fluids* 30 (2018) 033603.  
38  
39 [13] M. Discacciati, D. Hacker, A. Quarteroni, S. Quinodoz, S. Tissot, F. M.  
40 Wurm, Numerical simulation of orbitally shaken viscous fluids with  
41 free surface, *International Journal for Numerical Methods in Fluids* 71  
42 (2013) 294–315.  
43  
44 [14] M. Reclari, M. Dreyer, S. Tissot, D. Obreschkow, F. M. Wurm,  
45 M. Farhat, Surface wave dynamics in orbital shaken cylindrical con-  
46 tainers, *Physics of Fluids* 26 (2014) 052104.  
47  
48  
49  
50  
51  
52  
53  
54  
55  
56  
57  
58  
59  
60  
61  
62  
63  
64  
65

- 1  
2  
3  
4  
5  
6  
7  
8  
9  
10  
11  
12  
13  
14  
15  
16  
17  
18  
19  
20  
21  
22  
23  
24  
25  
26  
27  
28  
29  
30  
31  
32  
33  
34  
35  
36  
37  
38  
39  
40  
41  
42  
43  
44  
45  
46  
47  
48  
49  
50  
51  
52  
53  
54  
55  
56  
57  
58  
59  
60  
61  
62  
63  
64  
65
- [15] E. Olmos, K. Loubiere, C. Martin, G. Delaplace, A. Marc, Critical agitation for microcarrier suspension in orbital shaken bioreactors: Experimental study and dimensional analysis, *Chemical Engineering Science* 122 (2015) 545–554.
  - [16] I. Pieralisi, G. Rodriguez, M. Micheletti, A. Paglianti, A. Ducci, Microcarriers’ suspension and flow dynamics in orbitally shaken bioreactors, *Chemical Engineering Research and Design* 108 (2016) 198–209.
  - [17] J. Büchs, U. Maier, C. Milbradt, B. Zoels, Power consumption in shaking flasks on rotary shaking machines: I. power consumption measurement in unbaffled flasks at low liquid viscosity, *Biotechnology and Bioengineering* 68 (2000) 589–593.
  - [18] J. Büchs, S. Lotter, C. Milbradt, Out-of-phase operating conditions, a hitherto unknown phenomenon in shaking bioreactors, *Biochemical Engineering Journal* 7 (2001) 135–141.
  - [19] W. Klöckner, J. Büchs, Advances in shaking technologies, *Trends in Biotechnology* 30 (2012) 307–314.
  - [20] R. Hermann, M. Lehmann, J. Büchs, Characterization of gas–liquid mass transfer phenomena in microtiter plates, *Biotechnology and Bioengineering* 81 (2003) 178–186.
  - [21] W. A. Duetz, B. Witholt, Oxygen transfer by orbital shaking of square vessels and deepwell microtiter plates of various dimensions, *Biochemical Engineering Journal* 17 (2004) 181–185.
  - [22] S. D. Doig, S. C. Pickering, G. J. Lye, F. Baganz, Modelling surface aeration rates in shaken microtitre plates using dimensionless groups, *Chemical Engineering Science* 60 (2005) 2741–2750.
  - [23] H. Zhang, S. R. Lamping, S. C. Pickering, G. J. Lye, P. A. Shamlou, Engineering characterisation of a single well from 24-well and 96-well microtitre plates, *Biochemical Engineering Journal* 40 (2008) 138–149.
  - [24] M. Funke, S. Diederichs, F. Kensy, C. Müller, J. Büchs, The baffled microtiter plate: increased oxygen transfer and improved online monitoring in small scale fermentations, *Biotechnology and Bioengineering* 103 (2009) 1118–1128.

- 1  
2  
3  
4  
5  
6  
7  
8  
9 [25] A. Dürauer, S. Hobiger, C. Walther, A. Jungbauer, Mixing at the mi-  
10 croscale: Power input in shaken microtiter plates, *Biotechnology Journal*  
11 11 (2016) 1539–1549.  
12  
13  
14 [26] S. Tissot, M. Farhat, D. L. Hacker, T. Anderlei, M. Kühner,  
15 C. Comninellis, F. Wurm, Determination of a scale-up factor from mix-  
16 ing time studies in orbitally shaken bioreactors, *Biochemical Engineering*  
17 *Journal* 52 (2010) 181–186.  
18  
19  
20 [27] R.-K. Tan, W. Eberhard, J. Büchs, Measurement and characterization  
21 of mixing time in shake flasks, *Chemical Engineering Science* 66 (2011)  
22 440–447.  
23  
24 [28] G. Rodriguez, W. Weheliye, T. Anderlei, M. Micheletti, M. Yianneskis,  
25 A. Ducci, Mixing time and kinetic energy measurements in a shaken  
26 cylindrical bioreactor, *Chemical Engineering Research and Design* 91  
27 (2013) 2084–2097.  
28  
29  
30 [29] G. Rodriguez, T. Anderlei, M. Micheletti, M. Yianneskis, A. Ducci,  
31 On the measurement and scaling of mixing time in orbitally shaken  
32 bioreactors, *Biochemical Engineering Journal* 82 (2014) 10–21.  
33  
34  
35 [30] Y. Li, A. Ducci, M. Micheletti, Mixing time in intermediate-sized or-  
36 bitally shaken reactors with small orbital diameters, *Chemical Engi-  
37 neering & Technology* 42 (2019) 1611–1617.  
38  
39  
40 [31] S. Weiss, G. T. John, I. Klimant, E. Heinzle, Modeling of mixing in 96-  
41 well microplates observed with fluorescence indicators, *Biotechnology*  
42 *Progress* 18 (2002) 821–830.  
43  
44 [32] L. A. Melton, C. Lipp, R. Spradling, K. Paulson, Dismt-determination  
45 of mixing time through color changes, *Chemical Engineering Commu-  
46 nications* 189 (2002) 322–338.  
47  
48  
49 [33] N.-S. Cheng, Formula for the viscosity of a glycerol- water mixture,  
50 *Industrial & Engineering Chemistry Research* 47 (2008) 3285–3288.  
51  
52  
53 [34] R. A. Ibrahim, *Liquid sloshing dynamics: theory and applications*, Cam-  
54 bridge University Press, 2005.  
55  
56  
57  
58  
59  
60  
61  
62  
63  
64  
65



1  
2  
3  
4  
5  
6  
7  
8  
9  
10  
11  
12  
13  
14  
15  
16  
17  
18  
19  
20  
21  
22  
23  
24  
25  
26  
27  
28  
29  
30  
31  
32  
33  
34  
35  
36  
37  
38  
39  
40  
41  
42  
43  
44  
45  
46  
47  
48  
49  
50  
51  
52  
53  
54  
55  
56  
57  
58  
59  
60  
61  
62  
63  
64  
65

[35] D. F. Gerson, M. M. Kole, Quantitative measurements of mixing intensity in shake-flasks and stirred tank reactors: use of the mixmeter, a mixing process analyzer, *Biochemical Engineering Journal* 7 (2001) 153–156.

[36] H. Zhang, W. Williams-Dalson, E. Keshavarz-Moore, P. A. Shamlou, Computational-fluid-dynamics (cfd) analysis of mixing and gas-liquid mass transfer in shake flasks, *Biotechnology and Applied Biochemistry* 41 (2005) 1–8.

[37] G. Rodriguez, M. Micheletti, A. Ducci, Macro-and micro-scale mixing in a shaken bioreactor for fluids of high viscosity, *Chemical Engineering Research and Design* 132 (2018) 890–901.

1  
2  
3  
4  
5  
6  
7  
8  
9  
10  
11  
12  
13  
14  
15  
16  
17  
18  
19  
20  
21  
22  
23  
24  
25  
26  
27  
28  
29  
30  
31  
32  
33  
34  
35  
36  
37  
38  
39  
40  
41  
42  
43  
44  
45  
46  
47  
48  
49  
50  
51  
52  
53  
54  
55  
56  
57  
58  
59  
60  
61  
62  
63  
64  
65

Table 1: Summary of mixing time measurements carried out in shaken systems, ordered from the largest to the smallest reactor size.

	Ref.	Reactor geometry and size	Operating conditions	Measurement technique
Lab-scale	Rodriguez et al (2014) [29]	Three cylindrical vessels with $d_i = 70, 100$ and $130$ mm and two Erlenmeyer flasks with nominal volume of $1$ and $2$ L	$d_o = 25$ mm, $N = 90 - 210$ rpm	DISMT technique
	Gerson & Kole (2001) [35]	1 L Erlenmeyer flask	$N = 0 - 200$ rpm, $V_f = 540$ mL	Mixmeter probe
	Tan et al (2011) [27]	Three Erlenmeyer flasks with nominal volumes of $100, 250$ and $500$ mL	$d_o = 25 - 50$ mm, $N = 100 - 350$ rpm, $V_f = 10\%$ of the nominal volume	Single pH indicator colourimetric technique
	Zhang et al (2005) [36]	250 mL Erlenmeyer flask	$d_o = 20 - 60$ mm, $N = 100 - 300$ rpm, $V_f = 25 - 100$ mL	CFD simulation
	Tissot et al (2010) [26]	Cylindrical vessel with $d_i = 10, 13, 16, 28.7$ and $125$ cm	Various $d_o, N$ and $V_f$	DISMT technique
Rodriguez et al (2013) [28]	Cylindrical vessel with $d_i = 100$ mm	$d_o = 25$ mm, $N = 60 - 140$ rpm, $V_f = 235 - 550$ mL	DISMT technique	
Rodriguez et al (2018) [37]	Cylindrical vessel with $d_i = 100$ mm	$d_o = 25$ mm, $N = 100 - 200$ rpm, three viscosities	DISMT technique	
Li et al (2019) [30]	A cylindrical with $d_i = 40$ mm and a square vessel with side = $35.4$ mm	$d_o = 3, 15$ and $50$ mm, $N = 100 - 1000$ rpm, $h/d_i = 0.5, 0.75$ and $1$	DISMT technique	
Micro-scale	Zhang et al (2008) [23]	24- and 96-deep square well with $d_i = 17$ and $8$ mm, respectively	$d_o = 3$ mm, $N = 500 - 1500$ rpm	CFD simulation
	Weiss et al (2002) [31]	96-well with either round or flat bottom	$d_o = 12$ mm, $N = 500 - 900$ rpm, $V_f = 200 \mu\text{L}$	Fluorescence pH sensor and soluble pH indicators

1  
2  
3  
4  
5  
6  
7  
8  
9  
10  
11  
12  
13  
14  
15  
16  
17  
18  
19  
20  
21  
22  
23  
24  
25  
26  
27  
28  
29  
30  
31  
32  
33  
34  
35  
36  
37  
38  
39  
40  
41  
42  
43  
44  
45  
46  
47  
48  
49  
50  
51  
52  
53  
54  
55  
56  
57  
58  
59  
60  
61  
62  
63  
64  
65

Table 2: Geometrical characteristics of the two well mimics and list of operating conditions investigated

	Square well with conical bottom	Cylindrical well with flat bottom
<b>Internal Diameter</b>	17.1	15.6
$d_i$ [mm]		
<b>Fluid height</b>	6.9 - 20.8	15.7 - 26.2
$h_f$ [mm]		
<b>Fill volume</b>	2 - 6	3 - 5
$V_f$ [mL]		
<b>Fluid viscosity</b>	$10^{-4}, 10^{-5}, 10^{-6}$	—
$[m^2s^{-1}]$		

Table 3: Surfactant concentrations and values of surface tension measured by the tensiometer

Surfactant concentration $\text{mOLL}^{-1}$	Dilution factor	Dynamic surface tension $\text{mNm}^{-1}$
0	—	72.3
$3.47 \times 10^{-3}$	0	68.4
$3.47 \times 10^{-4}$	10	51.1
$6.94 \times 10^{-5}$	50	44.9
$3.47 \times 10^{-5}$	100	31.8

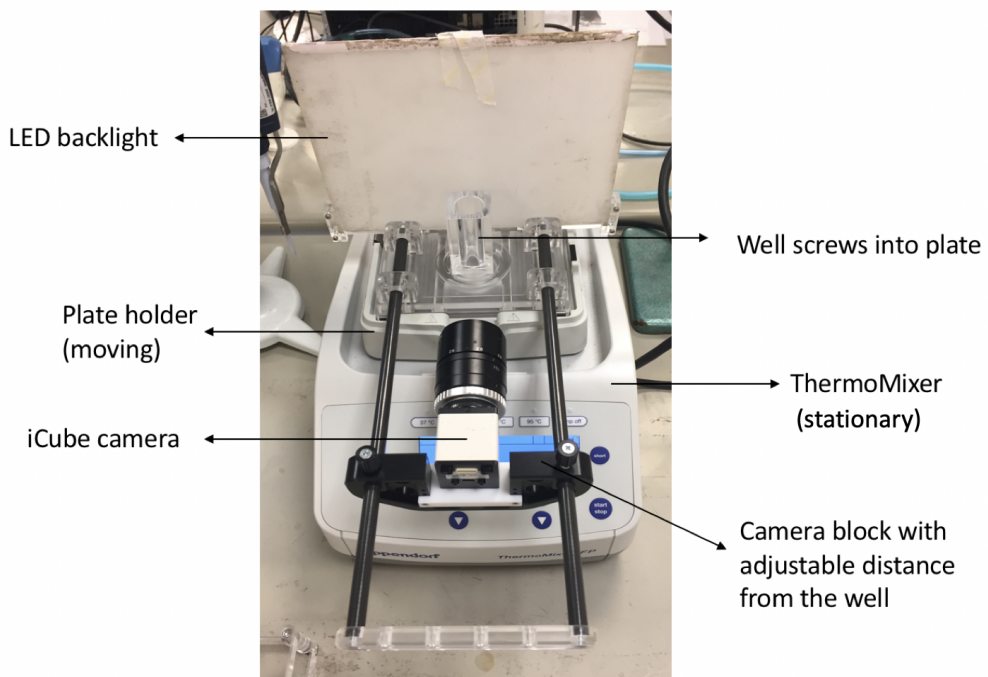


Figure 1: Set up for DISMT experiments on Eppendorf ThermoMixer C.

1  
2  
3  
4  
5  
6  
7  
8  
9  
10  
11  
12  
13  
14  
15  
16  
17  
18  
19  
20  
21  
22  
23  
24  
25  
26  
27  
28  
29  
30  
31  
32  
33  
34  
35  
36  
37  
38  
39  
40  
41  
42  
43  
44  
45  
46  
47  
48  
49  
50  
51  
52  
53  
54  
55  
56  
57  
58  
59  
60  
61  
62  
63  
64  
65

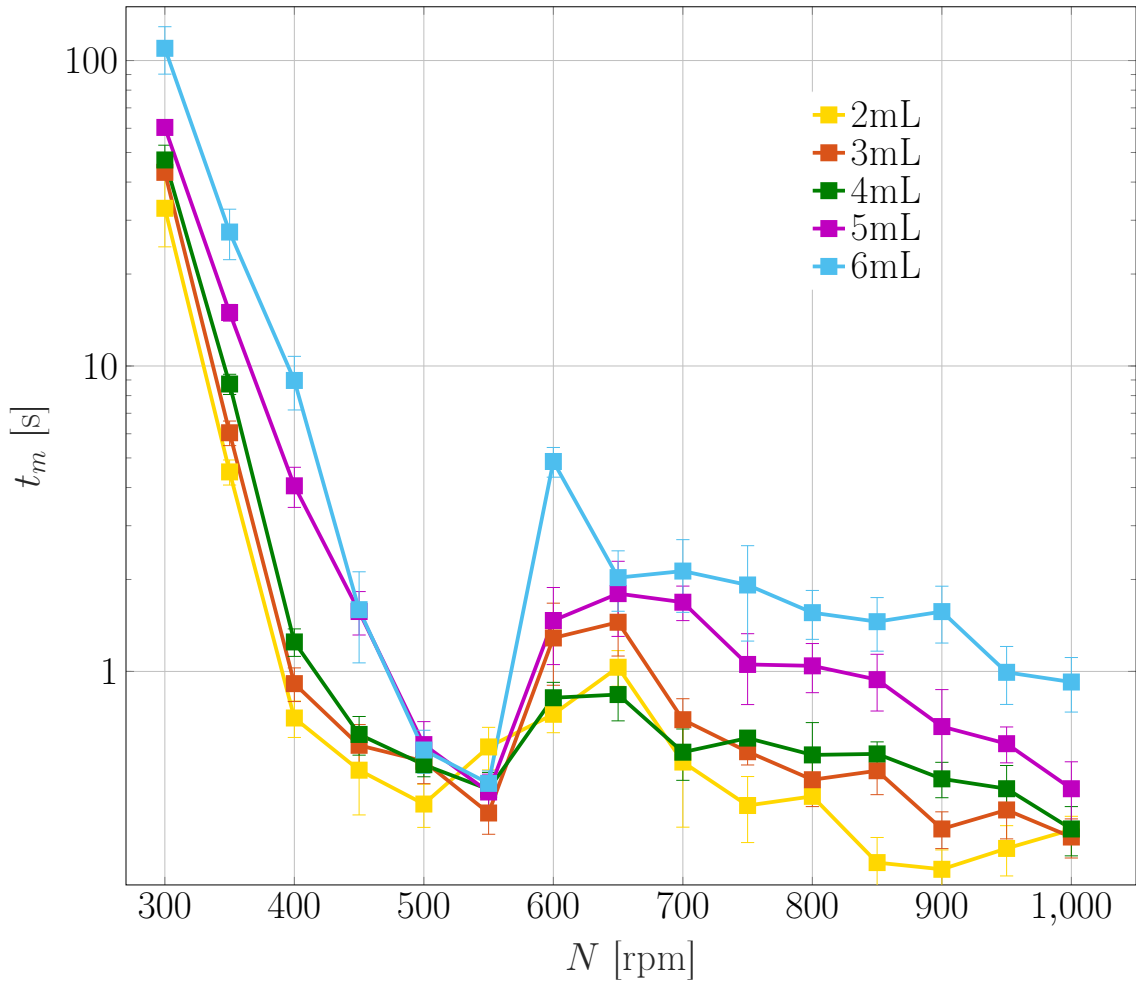


Figure 2: The effect of fill volume on mixing time in the 24-DSW format.

1  
2  
3  
4  
5  
6  
7  
8  
9  
10  
11  
12  
13  
14  
15  
16  
17  
18  
19  
20  
21  
22  
23  
24  
25  
26  
27  
28  
29  
30  
31  
32  
33  
34  
35  
36  
37  
38  
39  
40  
41  
42  
43  
44  
45  
46  
47  
48  
49  
50  
51  
52  
53  
54  
55  
56  
57  
58  
59  
60  
61  
62  
63  
64  
65

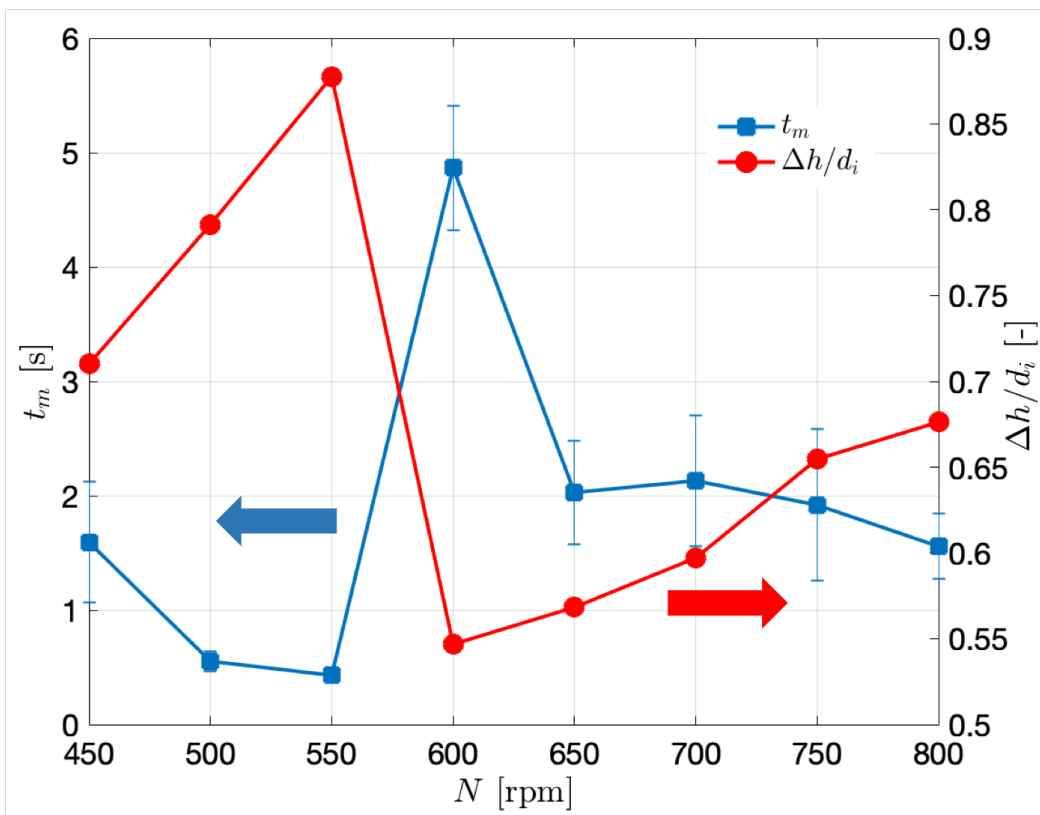


Figure 3: Comparison between mixing time and non-dimensional free surface amplitude in the square well with  $V_f = 6$  mL.

1  
2  
3  
4  
5  
6  
7  
8  
9  
10  
11  
12  
13  
14  
15  
16  
17  
18  
19  
20  
21  
22  
23  
24  
25  
26  
27  
28  
29  
30  
31  
32  
33  
34  
35  
36  
37  
38  
39  
40  
41  
42  
43  
44  
45  
46  
47  
48  
49  
50  
51  
52  
53  
54  
55  
56  
57  
58  
59  
60  
61  
62  
63  
64  
65

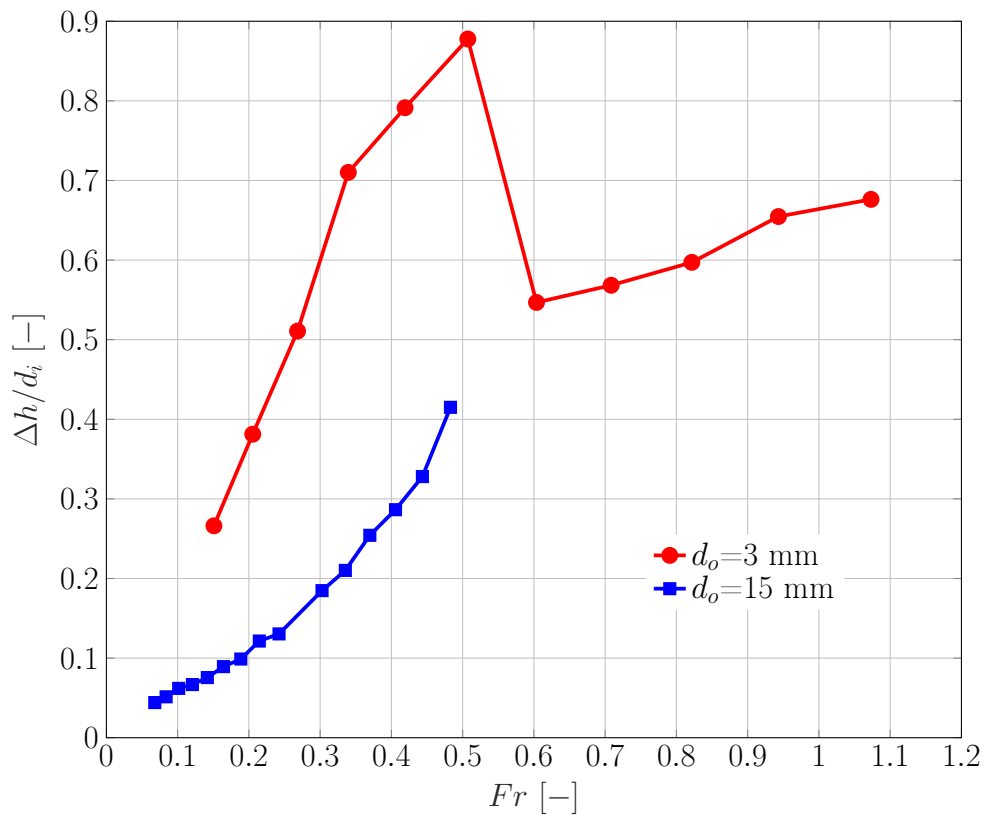


Figure 4: Non-dimensional free surface amplitude versus Froude number for two different orbital diameters in the square well with  $V_f = 6$  mL .

1  
2  
3  
4  
5  
6  
7  
8  
9  
10  
11  
12  
13  
14  
15  
16  
17  
18  
19  
20  
21  
22  
23  
24  
25  
26  
27  
28  
29  
30  
31  
32  
33  
34  
35  
36  
37  
38  
39  
40  
41  
42  
43  
44  
45  
46  
47  
48  
49  
50  
51  
52  
53  
54  
55  
56  
57  
58  
59  
60  
61  
62  
63  
64  
65

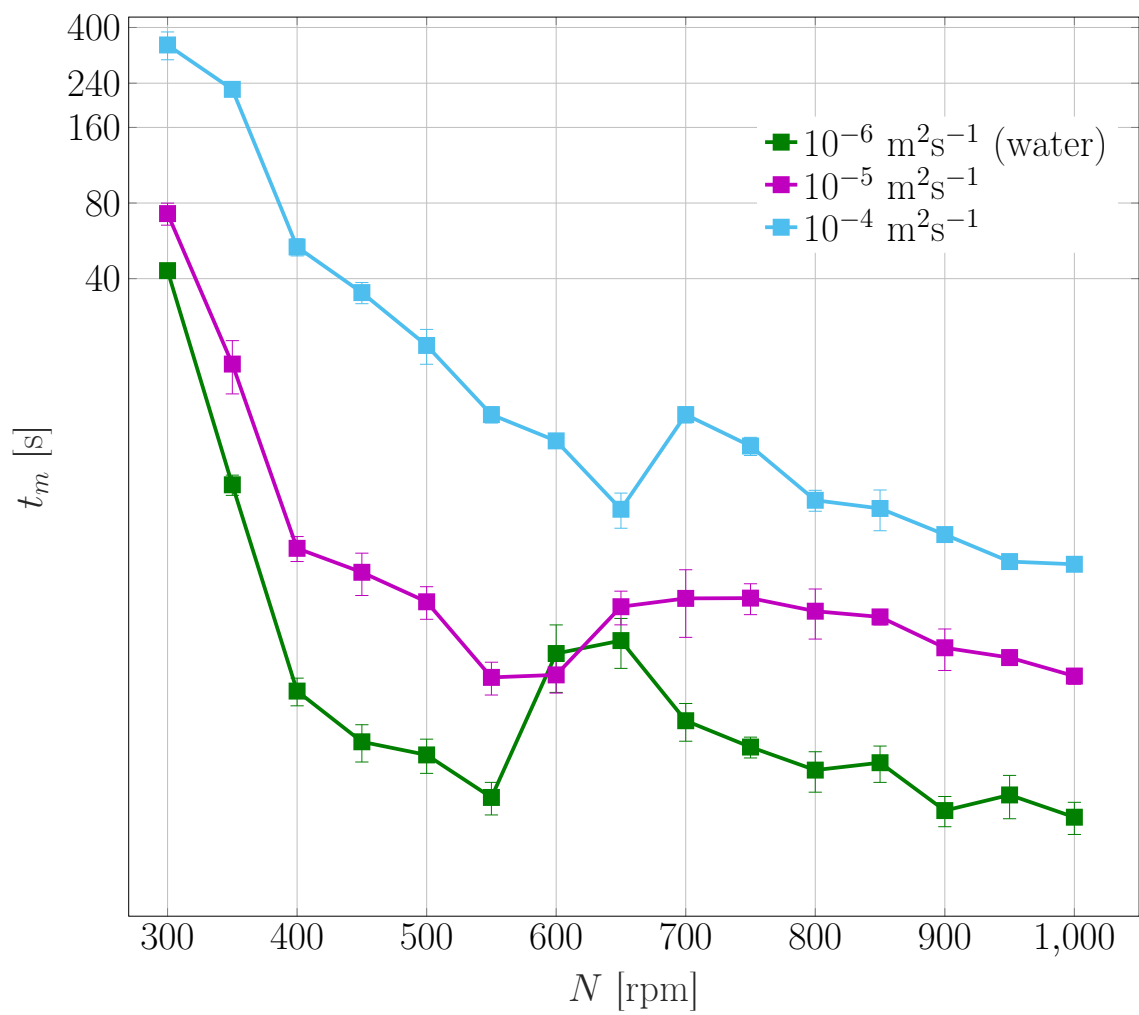


Figure 5: The effect of fluid viscosity on mixing time in the 24-DSW format with  $V_f=3$  mL.



1  
2  
3  
4  
5  
6  
7  
8  
9  
10  
11  
12  
13  
14  
15  
16  
17  
18  
19  
20  
21  
22  
23  
24  
25  
26  
27  
28  
29  
30  
31  
32  
33  
34  
35  
36  
37  
38  
39  
40  
41  
42  
43  
44  
45  
46  
47  
48  
49  
50  
51  
52  
53  
54  
55  
56  
57  
58  
59  
60  
61  
62  
63  
64  
65

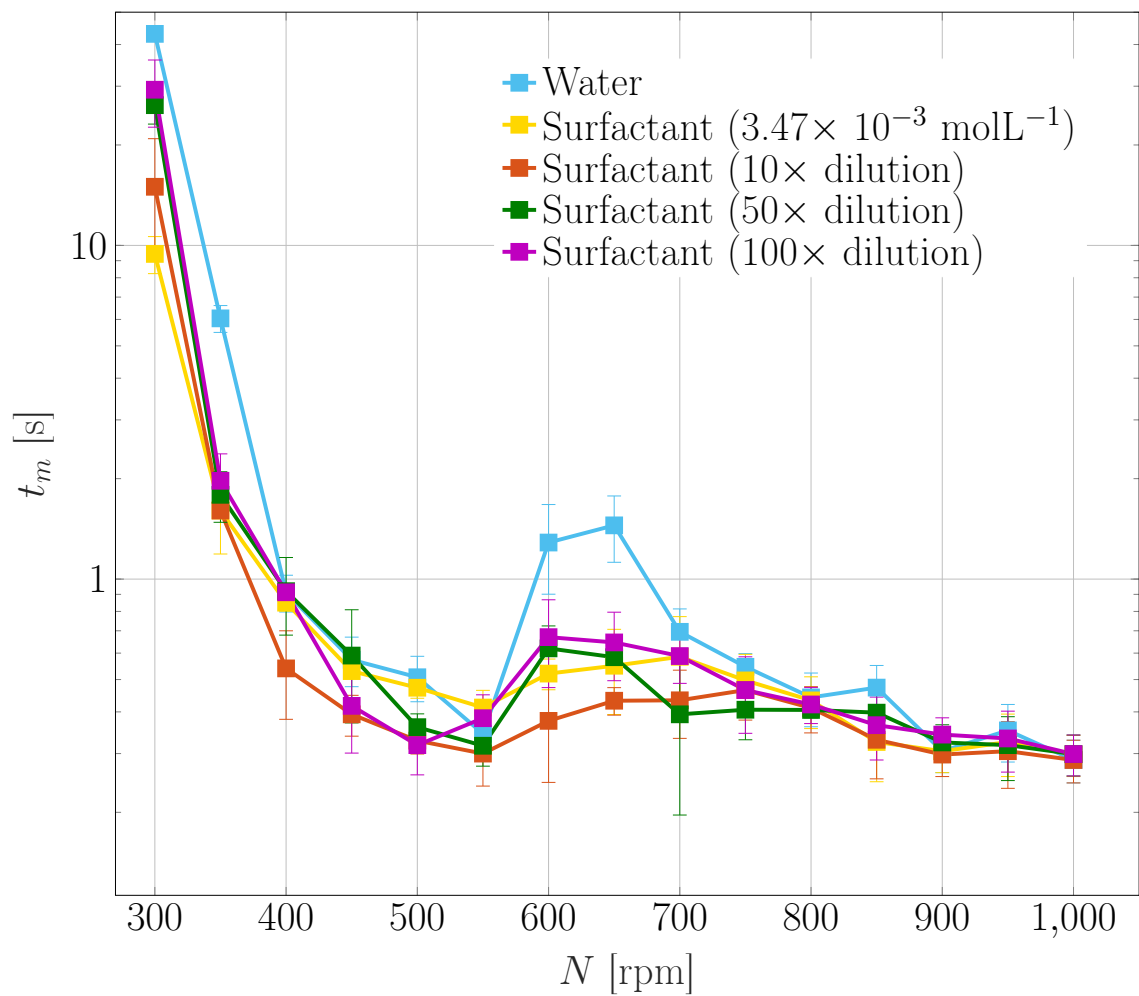


Figure 6: The effect of surface tension on mixing time in the 24-DSW format with  $V_f=3$  mL.

1  
2  
3  
4  
5  
6  
7  
8  
9  
10  
11  
12  
13  
14  
15  
16  
17  
18  
19  
20  
21  
22  
23  
24  
25  
26  
27  
28  
29  
30  
31  
32  
33  
34  
35  
36  
37  
38  
39  
40  
41  
42  
43  
44  
45  
46  
47  
48  
49  
50  
51  
52  
53  
54  
55  
56  
57  
58  
59  
60  
61  
62  
63  
64  
65

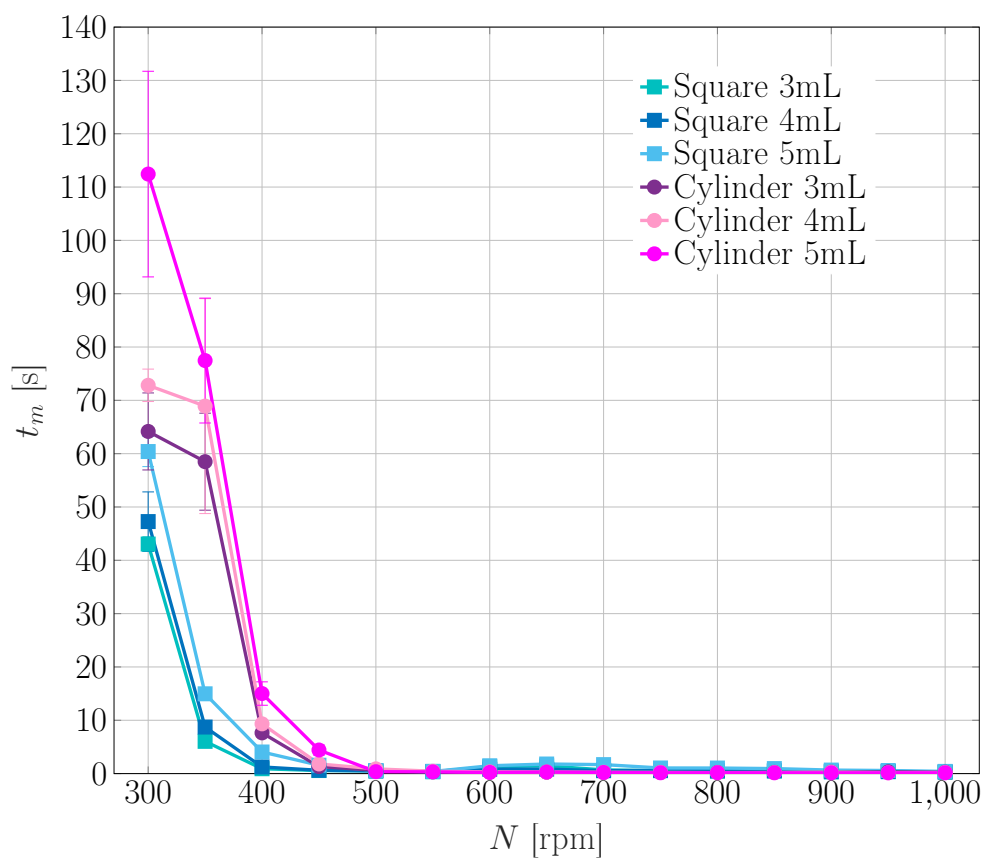
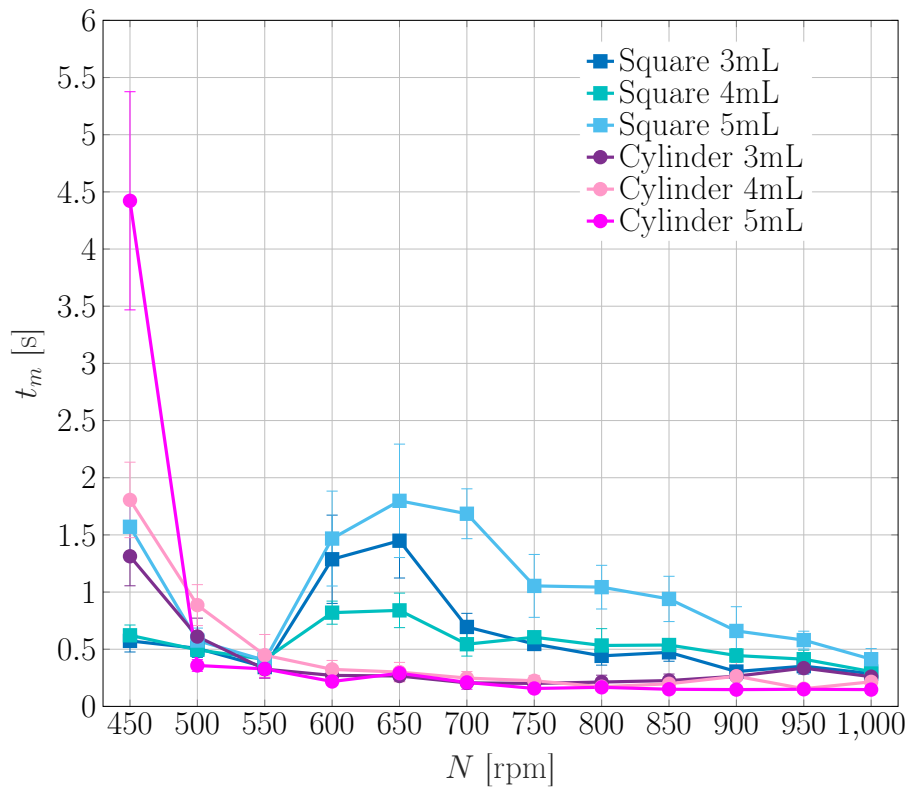
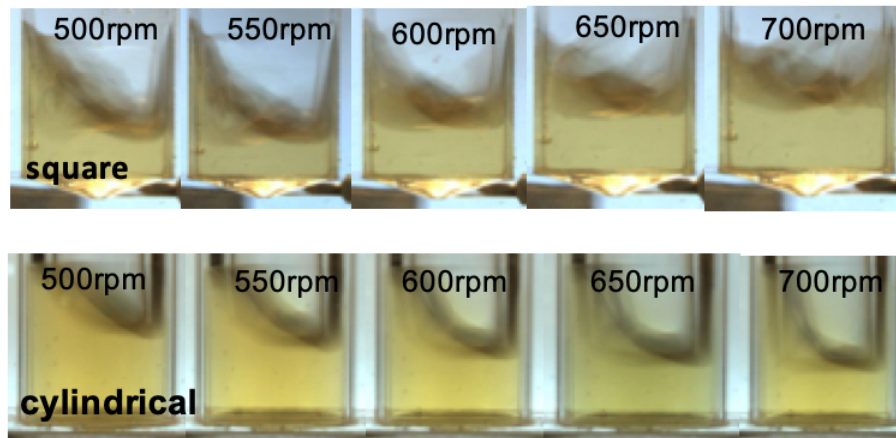


Figure 7: Comparison of mixing time variation with shaken speed between square and cylindrical geometries for three different fill volumes.



(a)



(b)

Figure 8: (a) Zoomed-in figure of the variation of mixing time with shaken speed in the range of 400 - 1000 rpm for square and cylindrical geometries. (b) Phase-locked images showing the difference of free surface shapes at certain speed ranges in the two geometries.

1  
2  
3  
4  
5  
6  
7  
8  
9  
10  
11  
12  
13  
14  
15  
16  
17  
18  
19  
20  
21  
22  
23  
24  
25  
26  
27  
28  
29  
30  
31  
32  
33  
34  
35  
36  
37  
38  
39  
40  
41  
42  
43  
44  
45  
46  
47  
48  
49  
50  
51  
52  
53  
54  
55  
56  
57  
58  
59  
60  
61  
62  
63  
64  
65

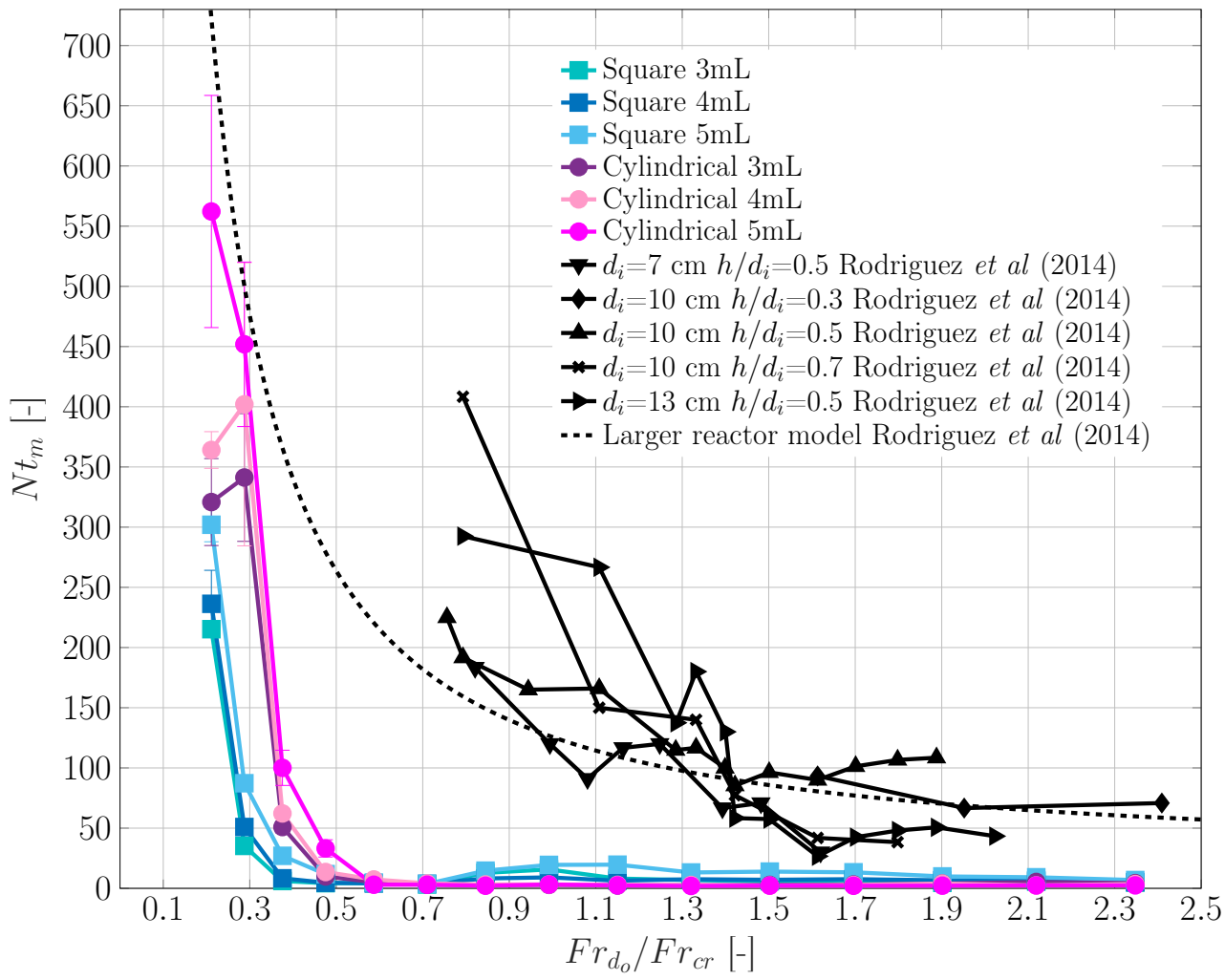


Figure 9: Comparison between present data with those reported by Rodriguez et al. [29] in terms of their proposed scaling parameter  $Fr/Fr_{cr}$ .

1  
2  
3  
4  
5  
6  
7  
8  
9  
10  
11  
12  
13  
14  
15  
16  
17  
18  
19  
20  
21  
22  
23  
24  
25  
26  
27  
28  
29  
30  
31  
32  
33  
34  
35  
36  
37  
38  
39  
40  
41  
42  
43  
44  
45  
46  
47  
48  
49  
50  
51  
52  
53  
54  
55  
56  
57  
58  
59  
60  
61  
62  
63  
64  
65

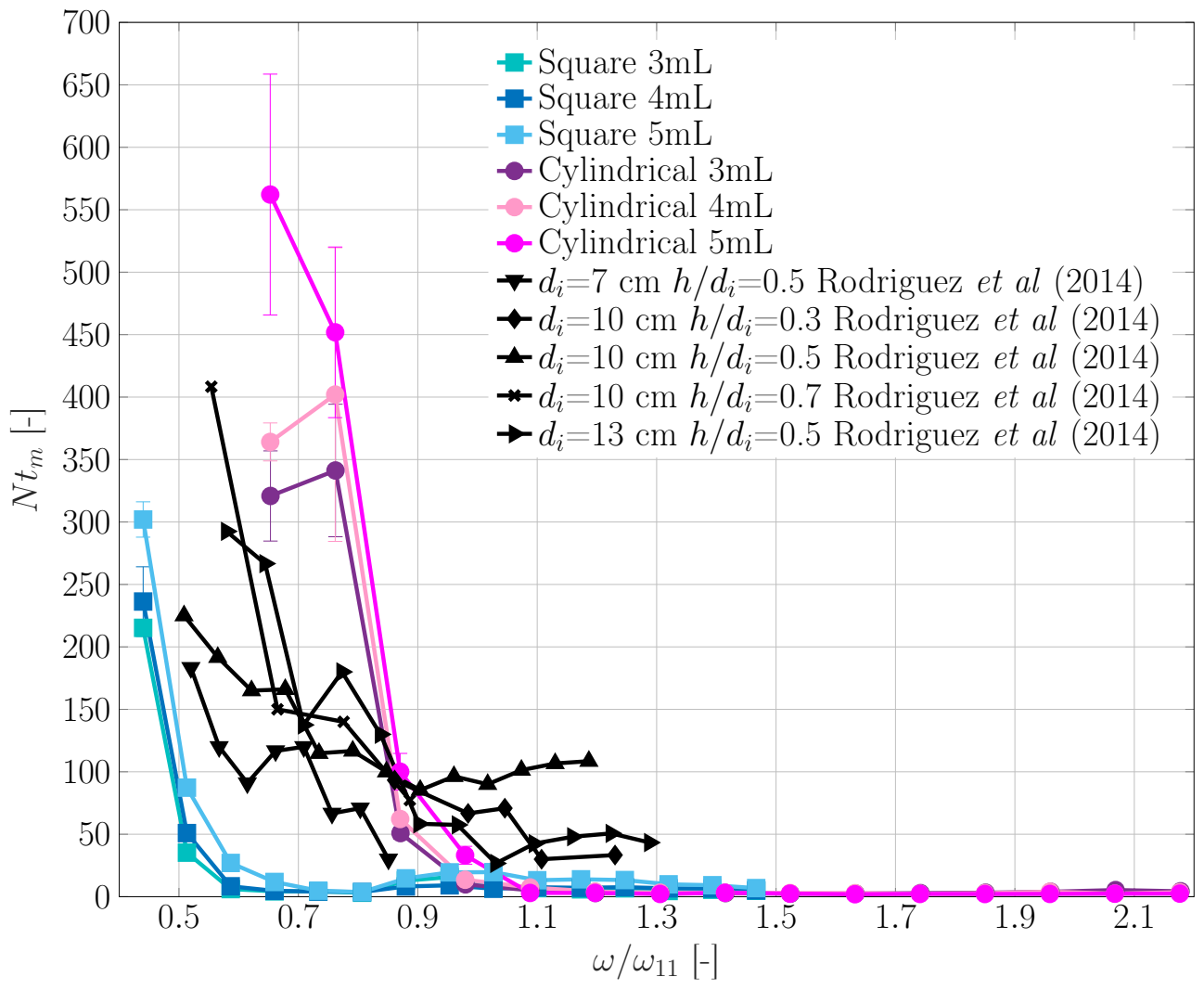


Figure 10: Comparison between present data with those reported by Rodriguez et al. [29] in terms of a new scaling parameter  $\omega/\omega_{11}$ .

**Source file**

[Click here to download Source file: Archieve\\_manuscript.rar](#)

[Click here to view linked References](#)